Self-focusing of few-cycle light pulses in dielectric media

Andrey N. Berkovsky, Sergei A. Kozlov, and Yuri A. Shpolyanskiy
St. Petersburg State University of Information Technology, Mechanics and Optics, 14 Sablinskaya street, St. Petersburg, 197101, Russia
(Received 25 February 2005; published 27 October 2005)

Various scenarios of self-focusing of axisymmetric few-cycle light pulses in optical media with nonresonant dispersion and nonlinearity are investigated numerically. It is shown that the spatiotemporal dynamics leads to the formation of complex light structures like dumbbells or bubbles depending on the initial intensity. The bubble includes a center area with emptiness, where the electrical field is practically nullified. An analysis is made of the characteristics of spectral supercontinuum generation accompanying the dispersive self-focusing. The development of a broad blueshifted spectral wing during the breakdown of a shock wave of the pulse profile is considered in detail.

DOI: 10.1103/PhysRevA.72.043821 PACS number(s): 42.65.Re, 42.65.Jx, 42.25.Fx

I. INTRODUCTION

Propagation of optical pulses containing approximately ten or fewer field cycles in transparent optical media has been attracting great experimental and theoretical interest since their first demonstration [1–3]. For the purposes of this work, let us label them as extremely short pulses (ESPs) associating the extreme brevity with the number of field oscillations rather than the pulse duration, *per se*. Theoretical models of ESP propagation having been actively discussed in recent years [4–6] differ from conventional models based on the slowly-varying-envelope approximation which was initially suggested for quasimonochromatic pulses with many field oscillations [7,8]. Nonlinear equations of ESP propagation are written directly for the pulse electrical field because the envelope approach becomes unnecessary for few-cycle regimes both analytically and numerically. The field equations are usually less complicated than their envelope analogs. For example, it is typical for active Raman media that a single field equation is transformed into a set of coupled equations for envelopes of pulses spectrally centered at pump and sequential Stokes and anti-Stokes frequencies [5,9].

The field dynamics of ESPs with an invariable transverse structure has been studied rather thoroughly (see Refs. [4–6] for a review as well as general analytical conclusions drawn for the motion of pulse averages [9]). This (1+1)-dimensional consideration is a first approximation in the analysis of ESP evolution in waveguides. It predicts that the spectral supercontinuum generation is immanent to ESP propagation and accompanies both the temporal self-compression and self-broadening of ESP as well as the formation of extremely short shock waves and solitons [5,9,10]. The phase self-modulation appears to be strong enough to produce octave-spanning spectra owing to the lack of optical breakdown in the few-cycle time scale even at very high intensities. Note that the bandwidth of a spectrally limited ESP is also comparable to the central frequency because of the pulse duration. These pulses are often produced just by the compression of femtosecond continua [1–3].

The supercontinuum generation can also be very effective when an intense femtosecond pulse experiences spatial self-focusing in a bulk medium [11]. The respective (3+1)-dimensional studies have been based on envelope equations (see, e.g., Refs. [2,12–14] and references therein). The authors demonstrated that self-focusing of femtosecond pulses has important special features as compared to that of longer (nano- or picosecond) pulses. For instance, the following self-focusing path becomes possible: a transverse pulse space constriction stimulates steepening of the pulse tail and a consequent turnover of the envelope shock wave gives rise to an intense blueshifted spectral wing [12]. However, the turnover leads to singularities in the pulse envelope thus seriously restricting the applicability of the approach while the field consideration remains self-consistent [10,15].

Here we analyze the paraxial spatiotemporal dynamics of the ESP electrical field in transparent isotropic nonlinear media. We present unidirectional field equations and discuss their advantages and disadvantages compared to the respective envelope equations. We develop a numerical model using the field consideration and simulate the evolution of ESPs with various initial intensities in media with normal group dispersion. The computations classify the ESP dynamics paths when either dumbbell-like spatiotemporal structures or bubblelike electromagnetic clots with few-wavelength-size emptinesses can be registered at the medium output. Our approach verifies the conclusion of Ref. [12] made on the base of the envelope consideration that the development of a broad blueshifted spectral pedestal during the dispersive self-focusing is induced by the steepening and a subsequent turnover of the pulse tail. We specially illustrate the detailed field and spectral dynamics in the area where the tail collapses.

II. EQUATION FOR THE PULSE ELECTRICAL FIELD

The spatiotemporal field dynamics in dielectric nonmagnetic optical media where self-focusing of ESPs is usually observed can be described by the equation

$$\nabla \times \nabla \times E + \frac{1}{c^2}\frac{\partial^2 D}{\partial t^2} = 0, \tag{1}$$

where E is the electrical field, D is the electric displacement vector, t is time, and c is the light velocity in vacuum.

Finite solutions of Eq. (1) satisfy Maxwell's Eq.

$$\nabla D = 0, \tag{2}$$

which can be checked by applying the divergence operator ∇ to Eq. (1) and taking into account the mathematical fact that $\nabla[\nabla \times A]=0$ for an arbitrary vector A.

We will address a nonresonant interaction of the light field with a dielectric medium when the pulse spectrum remains within the transparency band. The response of the medium which is additionally assumed to be homogeneous and isotropic to the electrical field can be written in the form [16]

$$D = \varepsilon E + D_{in} + D_{nl}, \tag{3}$$

where the first term describes the instant linear part of the displacement vector, the second term is for the inertial part, and the third one characterizes the nonlinear response. The value of the medium constant ε can be defined, e.g., as the dielectric permittivity taken at the initial central frequency of the pulse. The substitution of the representation (3) into Maxwell's equation (2) gives

$$\nabla E = -\frac{1}{\varepsilon} \nabla (D_{in} + D_{nl}). \tag{4}$$

Using the vector formula $\nabla \times \nabla \times = \nabla(\nabla \cdot) - \Delta$ and taking Eq. (4) into account, we can rewrite Eq. (1) into

$$\Delta E - \frac{\varepsilon}{c^2}\frac{\partial^2 E}{\partial t^2} - \frac{1}{c^2}\frac{\partial^2 D_{in}}{\partial t^2} - \frac{1}{c^2}\frac{\partial^2 D_{nl}}{\partial t^2} + \frac{1}{\varepsilon} \nabla (\nabla D_{in}) + \frac{1}{\varepsilon} \nabla (\nabla D_{nl}) = 0. \tag{5}$$

It should be noted that the following is valid for the terms of Eq. (3):

$$\varepsilon E \gg D_{in}, D_{nl}, \tag{6}$$

which explains the adequacy and usefulness of the representation (3). It is seen from the relation (6) that the defining wave character of the electrical field is described by the two leftmost terms of Eq. (5). Other terms are associated with the light dispersion or self-action and can generally have comparable orders of magnitude.

We restrict ourselves to the consideration of "wide" light beams with prohibited transverse field inhomogeneities of the central wavelength order and, respectively, a small longitudinal field component. Simple estimates then show that the two rightmost terms of Eq. (5) are much smaller than the third and fourth terms and, of course, the first two terms. For instance, the following is valid for any point in the medium bulk where induced oscillations of the displacement vector appear:

$$\frac{1}{c^2}\frac{\partial^2 D_{in,nl}}{\partial t^2} \sim \frac{D_{in,nl}^{max}}{(cT_c/4)^2}, \tag{7}$$

where $D_{in,nl}^{max}$ are maximum values of $D_{in,nl}$ and T_c is the period of oscillations related to the central pulse frequency. We can also estimate the order of the Cartesian components of the $\nabla(\nabla D_{in,nl})$ vectors:

$$\nabla(\nabla D_{in,nl})_j \sim \frac{\partial^2 (D_{in,nl})_i}{\partial j\, \partial i}, \frac{\partial^2 (D_{in,nl})_z}{\partial j\, \partial z}, \tag{8}$$

where z is the propagation distance; x and y are transverse coordinates; $i=x, y$; $j=x, y, z$. Assuming the beam to be wide as compared with the central wavelength $\lambda_c = cT_c$, i.e., requiring the relation

$$\frac{\partial^2 (D_{in,nl})_i}{\partial j\, \partial i}, \frac{\partial^2 (D_{in,nl})_z}{\partial j\, \partial z} \ll \frac{(D_{in,nl})_i}{(\lambda_c/4)^2} \tag{9}$$

to be satisfied at any time moment, we can reduce Eq. (5) to

$$\Delta E - \frac{\varepsilon}{c^2}\frac{\partial^2 E}{\partial t^2} - \frac{1}{c^2}\frac{\partial^2 D_{in}}{\partial t^2} - \frac{1}{c^2}\frac{\partial^2 D_{nl}}{\partial t^2} = 0. \tag{10}$$

Note that the requirement of a large beam width is sufficient but not necessary for the transition from Eq. (5) to Eq. (10). For example, the two rightmost terms in Eq. (5) turn to zero identically for (2+1)-dimensional linearly polarized waves. Self-focusing of ESPs with such dimensionality and polarization was studied in Ref. [17] for large transverse sizes and in Ref. [18] for transverse sizes comparable to the central wavelength. The nonparaxial evolution of (2+1)-dimensional linearly polarized monochromatic beams is discussed in Refs. [19,20].

The linear part of the dielectric permittivity ε_l defining the linear refractive index n_l will be supposed to vary polynomially with the optical frequency [21]:

$$\varepsilon_l(\omega) = n_L^2(\omega) = N_0^2 + 2cN_0 a\omega^2 - 2cN_0 \frac{b}{\omega^2}. \tag{11}$$

The dispersion law (11) follows from the Sellmeier formula and the assumption that the pulse frequencies are much lower than eigenfrequencies of an electronic subsystem in the dielectric and much higher than eigenfrequencies of an atomic subsystem, which formalizes the concept of transparency. The empirical constants N_0, a, and b can be fitted to describe adequately the nonresonant dispersion over an important part of the medium transparency band as well as a waveguide dispersion when it is necessary [5,9,10].

The nonlinear electronic response of an isotropic transparent dielectric to the ESP field can be written to a first approximation in the simplest form [5,22]

$$D_{nl} = \varepsilon_{nl}(E \cdot E)E, \tag{12}$$

where ε_{nl} is the nonlinear permittivity coefficient related to the nonlinear refractive index coefficient for a linearly polarized radiation via the ratio

$$n_2 = \frac{3\varepsilon_{nl}}{4N_0}. \tag{13}$$

We will neglect vibronic (Raman) nonlinearity due to its long response time as compared with a few-cycle duration [22,23]. A weakness of its effect on spectral ultrabroadening of femtosecond pulses is mentioned in Ref. [24]. The inertial accumulative part of plasma nonlinearity will also be ignored [2], but it should be noted that the instant contribution of this mechanism to n_2 is considerable and automatically accounted for in this constant [25] and, therefore, in the model

(12). For longer femtosecond pulses, the inertial part is very important: it can drastically effect on propagation of delayed field components [11,12], define existance of long filaments [13,14], and induce the optical breakdown [26].

The substitution of the medium response expressions (11) and (12) into Eq. (10) gives the following field equation:

$$\Delta E - \frac{N_0^2}{c^2}\frac{\partial^2 E}{\partial t^2} + \frac{2N_0}{c}a\frac{\partial^4 E}{\partial t^4} - \frac{2N_0}{c}bE - \frac{\varepsilon_{nl}}{c^2}\frac{\partial^2 (E\cdot E)E}{\partial t^2} = 0. \tag{14}$$

It can be easily checked that the linearized Eq. (14) incorporates the dispersion law (11) by considering its solutions as a superposition of monochromatic waves:

$$E = \frac{1}{2}e\mathcal{E}_\omega \exp[i(kz-\omega t)] + \text{c.c.}, \tag{15}$$

where $\mathcal{E}_\omega$ is the amplitude of a spectral component with the frequency ω, linearly polarized along the direction e, and $k(\omega)$ is the wave number. The notation (15) represents a solution to Eq. (14) if the dispersion of the linear refractive index $n_l(\omega)=(c/\omega)k(\omega)$ is defined by the expression (11).

The neglect of back-propagating waves associated with the assumption of a slowly varying field profile [4,5,7,27] allows one to reduce Eq. (14) to the integro-differential equation with a first-order z derivative

$$\frac{\partial E}{\partial z} + \frac{N_0}{c}\frac{\partial E}{\partial t} - a\frac{\partial^3 E}{\partial t^3} + b\int_{-\infty}^{t} E\,dt' + g\left[(E\cdot E)\frac{\partial E}{\partial t} + \frac{2}{3}E\times\left(E\times\frac{\partial E}{\partial t}\right)\right] = \frac{c}{2N_0}\Delta_\perp\int_{-\infty}^{t} E\,dt', \tag{16}$$

where $g=3\varepsilon_{nl}/2cN_0$, and $\Delta_\perp$ is the transverse Laplacian. The substitution of the representation (15) shows that the reduced equation describes the linear and nonlinear dispersion of the refractive index as

$$n(\omega) = N_0 + \Delta n_l(\omega) + \Delta n_{nl}(\omega), \tag{17}$$

where

$$\Delta n_l(\omega) = ca\omega^2 - c\frac{b}{\omega^2} \tag{18}$$

and

$$\Delta n_{nl}(\omega) = \tfrac{1}{2}n_2|\mathcal{E}_\omega|^2. \tag{19}$$

It is important to note that the decomposition (17) transforms the original nonresonant approximation (6) to the clear relation

$$N_0 \gg \Delta n_l(\omega), \Delta n_{nl}(\omega) \tag{20}$$

which is usually satisfied in the dispersive self-focusing of femtosecond pulses in transparent media.

The assumption of the slowly varying profile used in the derivation of Eq. (16) from Eq. (14) virtually replaces the dispersion law

$$n(\omega) = \sqrt{N_0^2 + 2N_0\Delta n_l(\omega)} \approx N_0 + \Delta n_l(\omega). \tag{21}$$

The validity of the transform follows evidently from the relation (20).

Equation (16) describes the dynamics of an arbitrarily polarized electrical field. Here we study self-focusing of linearly polarized ESPs and will analyze solutions of the scalar equation which is a special case of Eq. (16):

$$\frac{\partial E}{\partial z} + \frac{N_0}{c}\frac{\partial E}{\partial t} - a\frac{\partial^3 E}{\partial t^3} + b\int_{-\infty}^{t} E\,dt' + gE^2\frac{\partial E}{\partial t} = \frac{c}{2N_0}\Delta_\perp\int_{-\infty}^{t} E\,dt'. \tag{22}$$

Equation (22) with $a=b=g=0$ was derived in Ref. [28] for the analysis of ESP diffraction in vacuum. For a medium with dispersion and nonlinearity, it was first derived in Ref. [29] by a reduction of the complete wave equation coupled with a set of oscillator equations for electronic and vibronic polarizabilities. However the applicability limits of Eq. (22) were not discussed in Ref. [29]. The vector Eq. (16) was derived in Ref. [30] (see also Ref. [31]).

For the purposes of computations, it is convenient to rewrite Eq. (22) in normalized units by considering the retarded time $\tau=t-(c/N_0)z$ and scaled variables $\tilde{E}=E/E_0$, $\tilde{z}=a\omega_0^3 z$, $\tilde{y}=y/\Delta r$, $\tilde{x}=x/\Delta r$, and $\tilde{\tau}=\omega_0\tau$, where E_0,ω_0, and Δr are the initial pulse parameters defining the field maximum, the central frequency, and the transverse size, respectively. Substituting the variables, we can write Eq. (22) as

$$\frac{\partial E}{\partial z} - \frac{\partial^3 E}{\partial \tau^3} + B\int_{-\infty}^{\tau} E\,dt' + GE^2\frac{\partial E}{\partial \tau} = D\Delta_\perp\int_{-\infty}^{\tau} E\,d\tau', \tag{23}$$

where the tilde is omitted for simplicity and B,G, and D are effective dimensionless coefficients; $B=3(\omega_{cr}/\omega_0)^4$ and $\omega_{cr}=(b/3a)^{-4}$ is the frequency of zero group dispersion; $G=4\Delta n_{nl}/\Delta n_l$, where $\Delta n_{nl}=n_2E_0^2/2$ is actually the nonlinear contribution to the medium refractive index induced by a monochromatic wave with the amplitude E_0, and $\Delta n_l=ac\omega_0^2$ is the dispersion-induced contribution; and, finally, $D=c^2/2N_0\omega_0^2\Delta r^2\Delta n_l$. The values of coefficients B,G, and D depend on the medium characteristics and input pulse parameters and define what effects dominate at the initial propagation stage: normal or anomalous dispersion, nonlinear self-action, or diffraction.

III. THE FIELD EQUATION AS A GENERALIZATION OF ENVELOPE EQUATIONS

In this section we show that Eq. (22) generalizes known equations for envelopes of quasimonochromatic pulses [7,8] including their recent modifications to the case of few-cycle fields [32]. We start from the substitution

$$E(r,t) = \tfrac{1}{2}\mathcal{E}(r,t)\exp[i(k_0z-\omega_0t)] + \text{c.c.}, \tag{24}$$

where ω_0 is a fixed frequency, $k_0=\omega_0c/N_0$, and $\mathcal{E}(r,t)$ is a new variable for which Eq. (22) is rewritten as

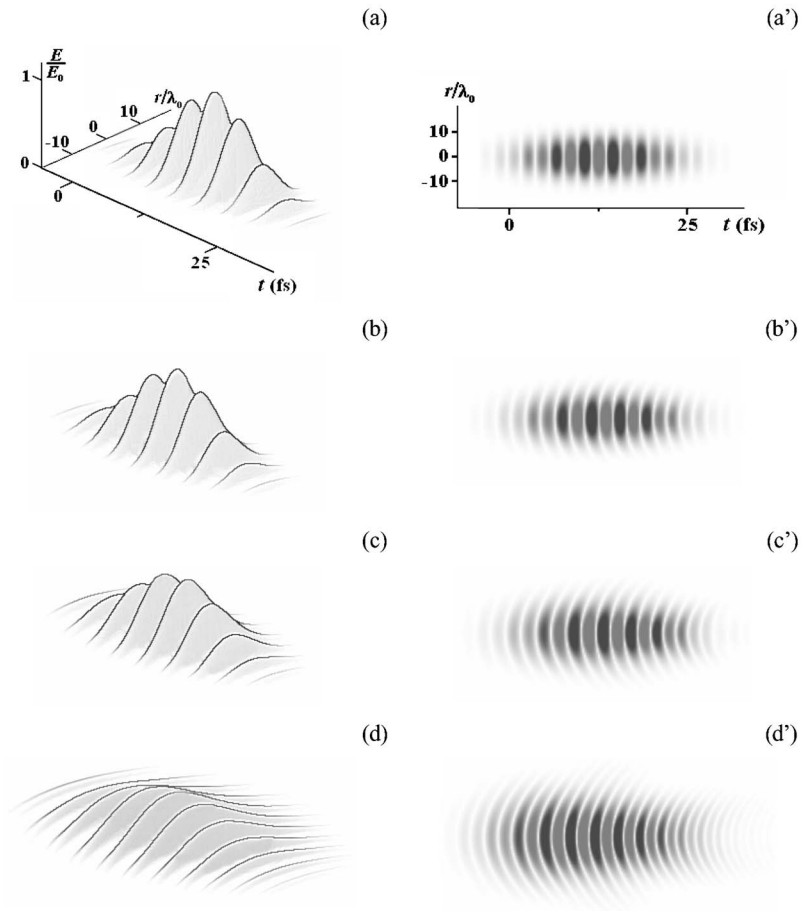

FIG. 1. The spatiotemporal dynamics of the ESP electrical field in bulk fused silica. The initial pulse parameters are $\lambda_0=780$ nm, $\Delta t=7.5$ fs, $\Delta r=10\lambda_0$, and $I=5\times10^{12}$ W/cm^2. The propagation distances are $z=$ (a), (a′) 0, (b), (b′) 0.1, (c), (c′) 0.2, and (d), (d′) 0.4 mm.

$$\frac{\partial\mathcal{E}}{\partial z}+\frac{1}{V}\frac{\partial\mathcal{E}}{\partial t}+i\frac{\beta_2}{2}\frac{\partial^2\mathcal{E}}{\partial t^2}-\frac{\beta_3}{6}\frac{\partial^3\mathcal{E}}{\partial t^3}-\sum_{n=4}^{\infty}\beta_n\frac{i^{n+1}}{n!}\frac{\partial^n\mathcal{E}}{\partial t''}-i\gamma_1|\mathcal{E}|^2\mathcal{E}$$
$$+\gamma_2\frac{\partial}{\partial t}(|\mathcal{E}|^2\mathcal{E})-\left(i\gamma_1\mathcal{E}^3+\gamma_2\mathcal{E}^2\frac{\partial\mathcal{E}}{\partial t}\right)\exp[2i(k_0z-\omega_0t)]$$
$$=\frac{i}{2k_0}\Delta_\perp\left(\frac{\omega_0}{i}\int_{-\infty}^{t}\mathcal{E}(r,t')\exp[i\omega_0(t-t')]dt'\right),\qquad(25)$$

where $V=(\partial k/\partial\omega)^{-1}_{\omega_0}$, $\beta_n=[\partial^n k(\omega)/\partial\omega^n]_{\omega_0}$, $k=(N_0/c)\omega+a\omega^3-b/\omega$, $\gamma_1=g\omega_0/4$, and $\gamma_2=g/4$.

Analyzing the evolution of quasimonochromatic pulses, it is natural to associate ω_0 with the carrier frequency and $\mathcal{E}(r,t)$ with the pulse envelope. If we keep in Eq. (25) only the third and fourth dispersion terms in the left-hand side, neglect the rightmost term which describes the generation of higher harmonics, and take only the first term in the expansion of the diffraction part in the right-hand side,

$$\frac{i}{2k_0}\Delta_\perp\left(\frac{\omega_0}{i}\int_{-\infty}^{t}\mathcal{E}(r,t')\exp[i\omega_0(t-t')]dt'\right)$$
$$=\frac{i}{2k_0}\Delta_\perp\left[\mathcal{E}(r,t)-\frac{i}{\omega_0}\frac{\partial\mathcal{E}(r,t)}{\partial t}+\left(\frac{i}{\omega_0}\right)^2\frac{\partial^2\mathcal{E}(r,t)}{\partial t^2}-\cdots\right],\qquad(26)$$

then Eq. (25) transforms to the known nonlinear equation for the pulse envelope [7,8]

$$\frac{\partial\mathcal{E}}{\partial z}+\frac{1}{V}\frac{\partial\mathcal{E}}{\partial t}+i\frac{\beta_2}{2}\frac{\partial^2\mathcal{E}}{\partial t^2}-\frac{\beta_3}{6}\frac{\partial^3\mathcal{E}}{\partial t^3}-i\gamma_1|\mathcal{E}|^2\mathcal{E}+\gamma_2\frac{\partial}{\partial t}(|\mathcal{E}|^2\mathcal{E})\mathcal{E}$$
$$=\frac{i}{2k_0}\Delta_\perp\mathcal{E}.\qquad(27)$$

The series (26) can be written out via the integration by parts.

The number of dispersion terms in (25) necessary for an adequate description of the $k(\omega)$ dependence increases for few-cycle fields with wide spectral bands. In addition, the diffraction term should be taken in its original integral form as in Eq. (25). In Ref. [32] it is written via the equivalent inverse operator

$$\frac{\omega_0}{i}\int_{-\infty}^{t}\mathcal{E}(r,z,t')\exp[i\omega_0(t-t')]dt'=\left(1+\frac{i}{\omega_0}\frac{\partial}{\partial t}\right)^{-1}\mathcal{E}(r,z,t).\qquad(28)$$

One can check the validity of the representation (28) by applying the forward operator $[1+(i/\omega_0)\partial/\partial t]$ to its left- and right-hand sides.

The rightmost term on the left-hand side of Eq. (25) is always ignored in the envelope approach because the aim of the method is to avoid the consideration of "fast" field oscillations inside the envelope. It means that even though the linearized Eqs.(22) and (25) are entirely equivalent, the complete nonlinear form of the latter ignores generation of multiple frequencies and their interaction with principal pulse

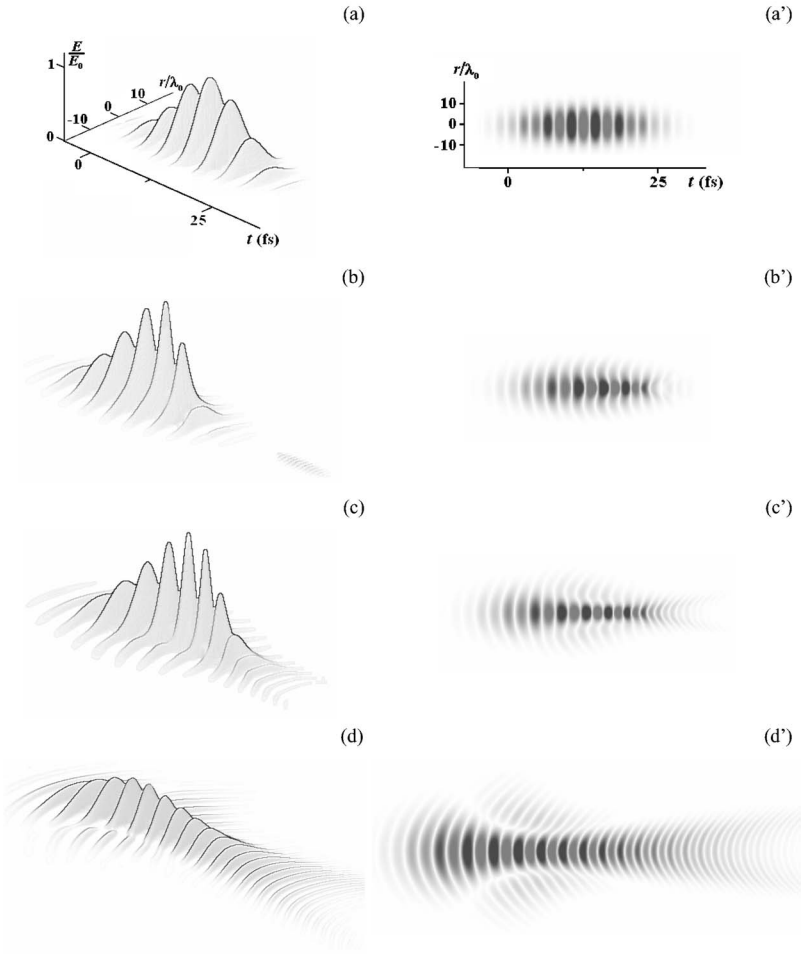

FIG. 2. The spatiotemporal dynamics of the ESP electrical field in bulk fused silica. The initial pulse parameters are $\lambda_0 = 780$ nm, $\Delta t = 7.5$ fs, $\Delta r = 10\lambda_0$, and $I = 1.5 \times 10^{13}$ W/cm^2. The propagation distances are $z =$ (a), (a′) 0, (b), (b′) 0.1, (c), (c′) 0.2, and (d), (d′) 0.4 mm.

frequencies. The multiple frequencies can be described only by additional envelope equations. In addition, the envelope approach loses its fundamental advantage over the field consideration when applied to ESPs because the pulse duration becomes comparable to the time scale of the field oscillations. The loss of the physical essence of the envelope concept manifests itself in a serious complication of Eq. (25) as compared to Eq. (27) and even the field Eq. (22) generalizing Eq. (25). Our simulations of the paraxial self-focusing of ESPs in dispersive nonlinear transparent media are based on Eq. (23), the normalized form of Eq. (22).

IV. SELF-FOCUSING OF FEW-CYCLE LASER PULSES IN FUSED SILICA

Figures 1–5 illustrate the field dynamics of an axisymmetric few-cycle pulse obtained via the numerical integration of Eq. (23). Our computations are based on the split-step Fourier-transform technique [8], when the effect of linear terms is calculated in the frequency domain, while nonlinearities are accounted for in the time domain. We apply the fast Fourier transform to the linear step and the Crank-Nicholson scheme to the nonlinear one. To controll the results, we check conservation of the pulse "energy" $W(z) = \int E^2(t,x,y,z)dt\,dx\,dy$ during propagation and compare distributions obtained on sequentially refined grids.

The input pulse profile is taken in the form

$$E(z,r,t)_{z=0} = E_0 \exp\left(-2\frac{r^2}{\Delta r^2}\right)\exp\left(-2\frac{t^2}{\Delta t^2}\right)\cos(\omega_0 t), \tag{29}$$

where $\lambda_0 = 2\pi c/\omega_0 = 780$ nm is the central wavelength of a Ti:sapphire laser, $\Delta t = 7.5$ fs is the pulse duration, $\Delta r = 10\lambda_0$ is the transverse size, and E_0 is the field maximum related to the radiation intensity I as E_0^2 (cgs electrostatic units) $= (8\pi/3N_0)I$ (kW/cm^2) [7]. The considered intensities are in the range of 5×10^{12}–2.5×10^{13} W/cm^2. The medium parameters are taken as those of fused silica with $N_0 = 1.4508$, $a = 2.7401 \times 10^{-44}$ s^3 cm^{-1}, $b = 3.9437 \times 10^{17}$ s^3 cm^{-1}, and $\tilde{n}_2 = 2.9 \times 10^{-13}$ cm^2/kW [$\tilde{n}_2$ (cm^2/kW) $= (4\pi/3N_0)n_2$ (cgs) (electrostatic units)] [10,22]. The values of effective coefficients for the parameters are $B = 0.422$, $D = 0.018$, and G in the range of 0.604–3.020.

Figures 1–3 present variation of the field spatiotemporal distribution during propagation. Three-dimensional axonometric views of the electrical field E normalized to its initial maximum E_0 are shown in Figs. 1–3 parts (a)–(d) as functions of time t and the transverse coordinate r normalized to

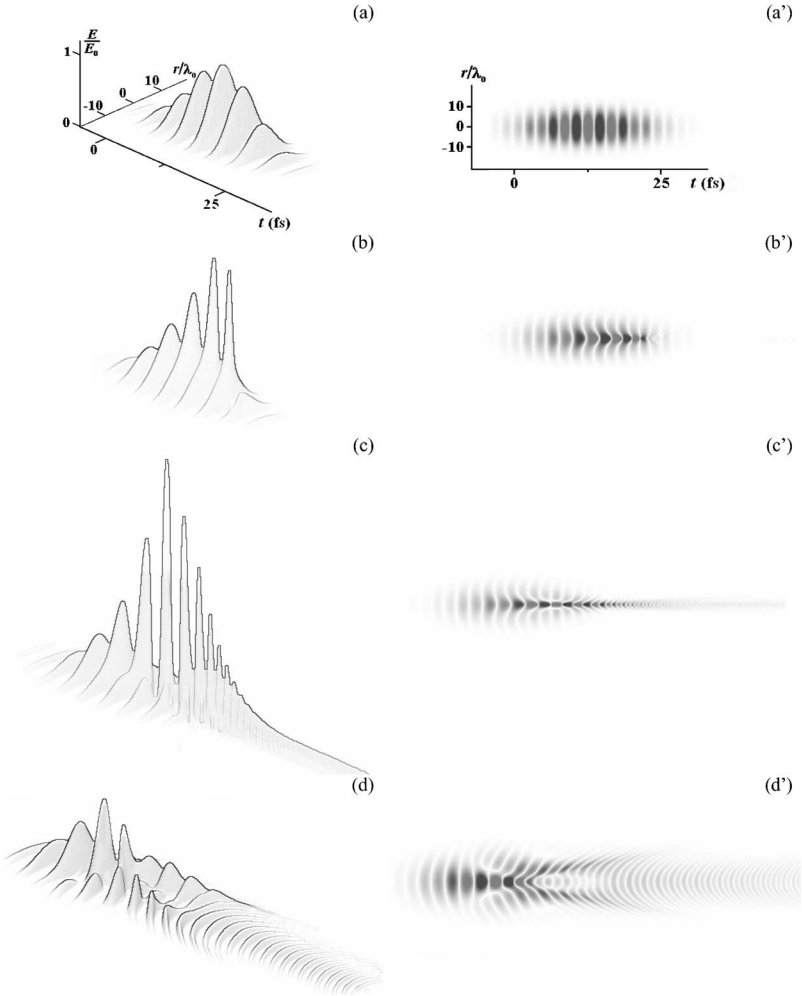

FIG. 3. The spatiotemporal dynamics of the ESP electrical field in bulk fused silica. The initial pulse parameters are $\lambda_0=780$ nm, $\Delta t=7.5$ fs, $\Delta r=10\lambda_0$, and $I=2.5\times10^{13}$ W/cm^2. The propagation distances are $z=$ (a), (a′) 0, (b), (b′) 0.05, (c), (c′) 0.1, and (d), (d′) 0.2 mm.

the initial central wavelength λ_0. Negative values of the electrical field hidden below the detached plane $E=0$ are symmetric to depicted positive values. In addition, Figs. 1–3 parts (a′)–(d′) give two-dimensional contour plots of the E distribution illustrating spatial wave fronts more clearly. Light and dark gray areas in Figs. 1–3 parts (a′)–(d′) represent maximum positive and negative E values, respectively.

Figure 1 gives the ESP dynamics at $I=5\times10^{12}$ W/cm^2 ($G=0.604$). One can see that the initial pulse intensity is insufficient for dramatic nonlinear effects. The pulse experiences a dispersion-induced temporal and diffraction-induced spatial broadening accompanied by a wave front curvature typical for the normal group dispersion.

Figures 2(a) and 2(d) and 2(a′)–2(d′) illustrate the spatiotemporal evolution of ESPs with parameters identical to those of Fig. 1 except for the higher peak intensity $I=1.5\times10^{13}$ W/cm^2 ($G=1.812$), which makes nonlinear effects appreciable. It is seen from Fig. 2(b) that self-focusing dominates first giving rise to the axial field amplitude primarily around the pulse center. The induced phase shift in the axial quasifilament is considerably higher than that in the periphery: by π at $z=0.05$ mm and more than 2π at

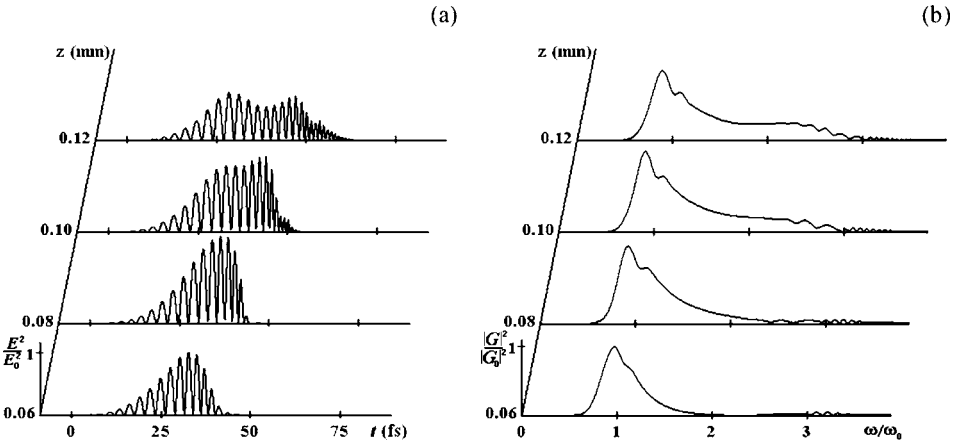

FIG. 4. The formation and breakdown of an axial envelope shock wave in bulk fused silica: the ESP electrical field E(a) and spectral density $|G|$ (b). The initial pulse parameters are $\lambda_0=780$ nm, $\Delta t=7.5$ fs, $\Delta r=10\lambda_0$, and $I=2.5\times10^{13}$ W/cm^2.

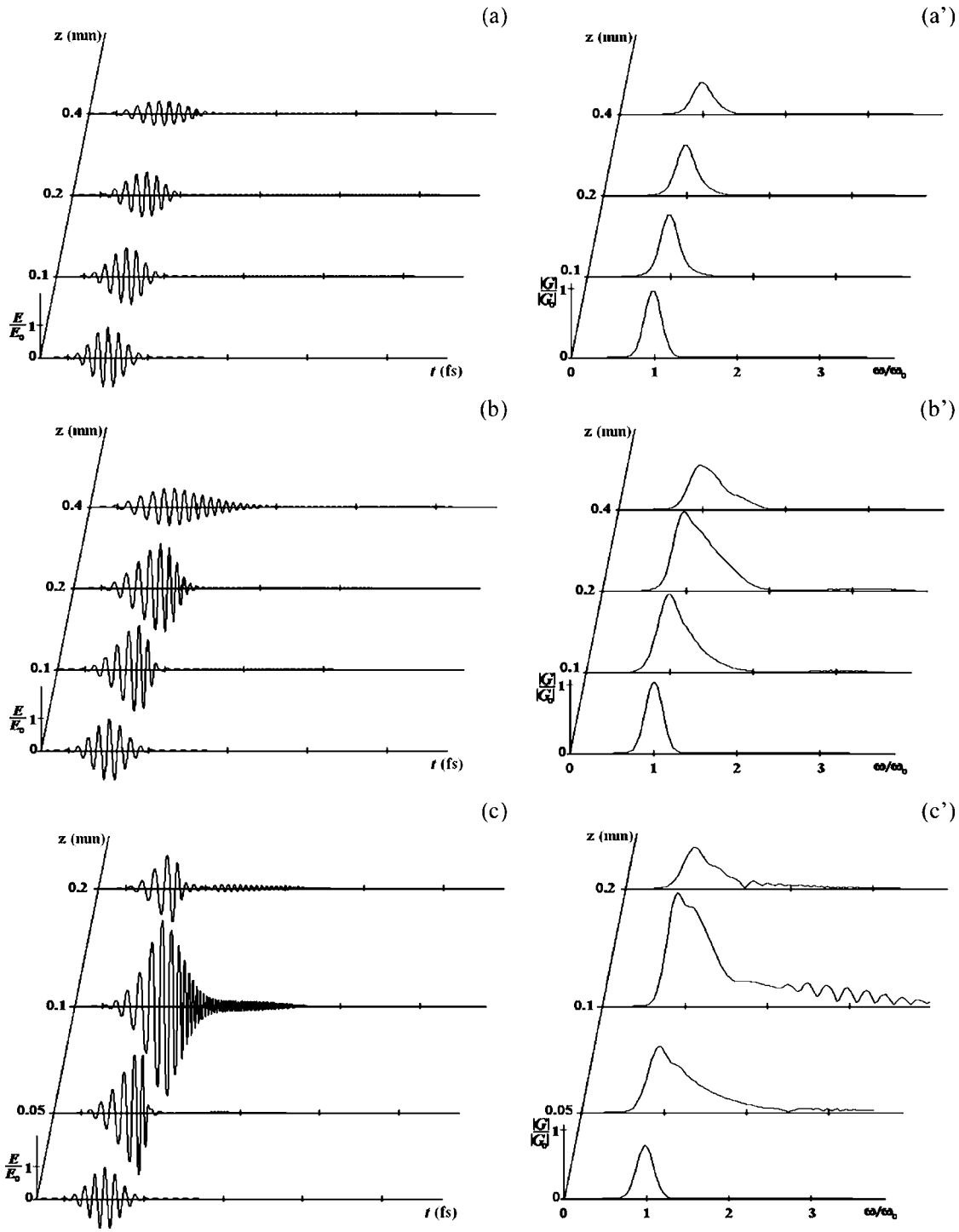

FIG. 5. The axial dynamics of the ESP electrical field E (a)–(c) and spectral density $|G|$ (a′)–(c′) in bulk fused silica. The input peak intensities are I= (a), (a′) 5×10^{12}, (b), (b′) 1.5×10^{13}, and (c), (c′) 2.5×10^{13} W/cm^2.

z=0.1 mm as presented in Figs. 2(b) and 2(c), respectively. Another nonlinear effect is the generation of a third-harmonic pulse, which splits from the basic frequencies and lags behind due to a difference in propagation rates defined by the group dispersion as shown in Fig. 2(b).

The increased field in the main body intensifies the nonlinear temporal broadening additional to the dispersion-induced one [Figs. 2(c) and 2(c′)]. The field distribution now looks like a nonsymmetric dumbbell noticeably stretched in time. Its front part is composed of low and the tail part of high frequencies. One can say that a narrow, intense waist with planar phase fronts connects two distinct subpulses separated both spatially and spectrally. The waist appears to be surrounded by a light ring with slightly different frequencies. A sequential amplitude decrease due to the temporal broadening leads to the quasilinear expansion of the dumbbell under the effects of diffraction and dispersion as shown in Figs. 2(d) and 2(a′). This self-focusing scenario seems to

be an analog of splitting of femtosecond pulses with many field oscillations into two shorter pulses (see, e.g., Ref. [33] and references herein). A field distribution similar to the dumbbell was called "butterfly shaped" in Ref. [34], where ESP self-action was simulated on the base of the modified nonlinear Schrödinger equation for envelopes.

The spatiotemporal evolution of even more intense ESP with $I=2.5\times10^{13}$ W/cm^2 ($G=3.020$) is illustrated in Figs. 3(a)–3(d) and 3(a′)–(3d′). Two self-focusing stages can be distinctly revealed now: prefocal and postfocal. The former is associated with the paraxial field increase [see Fig. 3(b)], more pronounced than in the previous case. Figure 3(b′) shows that the focusing region is shifted toward the pulse tail. The waist also appears, but now it resembles a thin channel with a clearly seen focal zone. The channel width decreases down to the wavelength order and the peak intensity rises up to the values about 10^{15} W/cm^2 [see Figs. 3(c) and 3(c′)]. Strictly speaking, this regime appears to be beyond the scope of the approximations used in the derivation of Eq. (22). First, the condition of the paraxial evolution (9) is violated. Second, the model of the nonlinear medium response (12) ceases to be valid for such intense fields. However, the analysis of the nonparaxial evolution shows that its scenario is similar to a first approximation to that observed in the paraxial case for regimes with the beam transverse focusing down to the order of 1–2 central wavelengths [18,20], while the plasma nonlinearity which becomes important for strong fields is inertial in the time scale of a few light oscillations [2]. So we will discuss subsequent computations, but considering the conclusions only as qualitative.

It should be noted that an infinite field increase (or "collapse") predicted, e.g., in Ref. [34] on the base of the envelope approach was not observed in our numerical experiments for the considered range of intensities, which was especially checked on refined computation grids. We did not analyze the possibility of collapse at initial intensities $I>2.5\times10^{13}$ W/cm^2 within the framework of the mathematical model (22), because the longitudinal field component becomes important for focused beams narrower than that presented in Fig. 3 and diffraction-imposed self-reflection should be accounted for [10,20]. Figure 4 presents the detailed axial dynamics of the squared electrical field and spectral amplitude around the focal point. It is seen that the intensity rise supports an essential steepening of the tail of the pulse "envelope" defined, e.g., as a curve connecting the field maxima, and then leads to the breakdown of this "envelope shock wave" with a sharp intensity decrease and generation of high-frequency components. Then the pulse duration increases and the axial intensity diminishes in favor of the periphery and practically nullifies in the center area as shown in Fig 3(d). Thus a light bubble field structure with a central emptiness is formed in the postfocal stage. Further, the bubble broadens quasilinearly due to diffraction and dispersion. High-frequency components produced at the moment of the shock wave turnover lag behind, forming the pulse tail. The bubble front is composed of low-frequency components. Note that the term light bubble is used in Ref. [35] for (1+1)-dimensional spatiotemporal video pulses which cannot be considered as electromagnetic clots with emptiness.

In Figs. 5(a)–5(c) and 5(a′)–5(c′) we additionally present the axial distributions of the electrical field E and its spectral amplitude $|G|$ normalized to their initial peak values E_0 and $|G_0|$ for all the computations. Figures 5(a) and 5(a′) illustrate that new frequencies are practically not generated in the quasilinear regime and the pulse spectrum remains unchanged, in contrast to the temporarily broadened field profile. The spectrum of the pulse with the initial peak intensity $I=1.5\times10^{13}$ W/cm^2 acquires new blueshifted frequencies during propagation as is seen from Fig. 5(b′). A comparison of Figs. 5(a) and 5(b) shows that self-focusing imposes an additional nonlinear temporal lens which doubles the ESP duration at the distance $z=0.4$ mm.

The highest considered intensity $I=2.5\times10^{13}$ W/cm^2 produces an extreme strengthening of the axial field with a subsequent steepening of the pulse tail, clearly seen in Fig. 5(c). The spectrum presented in Fig. 5(c′) experiences dramatic nonlinear changes broadening nonsymmetrically to both the low- and high-frequency sides. The development and turnover of the envelope shock wave, which was considered in detail in Fig. 4, gives rise to a broad blueshifted pedestal in the frequency domain. The phenomenon is known from experiments on self-focusing of femtosecond pulses with many field oscillations and agrees with qualitative predictions made on the base of the envelope approach [12].

V. CONCLUSION

We have demonstrated that the consideration of forward-propagating light fields is mathematically justified and useful in the analysis of the paraxial self-focusing of few-cycle laser pulses in transparent bulk media. The applicability limits of nonlinear envelope equations with various modifications, often applied even in the few-cycle time scale are written out by means of the more general field equation. The thought is expressed that the accuracy loss introduced by the envelope approach is not returned by computational advantages because of a very short pulse duration.

Using the field consideration, we simulated propagation of axisymmetric three-cycle pulses spectrally centered at 780 nm in bulk fused silica. It is shown that the nonlinear regimes lead to the formation of ultrashort light structures like dumbbells or bubbles depending on the initial intensity. The bubble includes a center area with emptiness, where the field is practically nullified. The field collapse was not observed in self-focusing for initial intensities up to $I=2.5\times10^{13}$ W/cm^2.

We especially addressed the process of the pulse tail steepening and subsequent turnover of the envelope shock wave and illustrated dramatic field and spectral changes. Our computations confirm that the development of a broad blueshifted spectral wing in the generating continuum is associated with the envelope breakdown as was suggested in Ref. [12] on the base of an approach only partially applicable to the analysis of shock-wave effects.

ACKNOWLEDGMENTS

This work was done within the framework of Project No. UR.01.01.047 of the scientific program "Universities of Russia" funded by the Ministry of Education and Science of the Russian Federation and Project No. 05-02-16556 of the Russian Foundation for Basic Research. Y.A.S. acknowledges the support of the Dynasty Foundation, Moscow, Russia.

[1] G. Steinmeyer, D. H. Sutter, L. Gallman, N. Matuschek, and U. Keller, Science **286**, 1507 (1999).
[2] Th. Brabec and F. Krausz, Rev. Mod. Phys. **72**, 545 (2000).
[3] G. Cerullo, S. De Silvestri, M. Nisoli, S. Sartania, S. Stagira, and O. Svelto, IEEE J. Quantum Electron. **6**, 948 (2000).
[4] A. I. Maimistov, Quantum Electron. **30**, 287 (2000).
[5] V. G. Bespalov, S. A. Kozlov, Yu. A. Shpolyansky, and I. A. Walmsley, Phys. Rev. A **66**, 013811 (2002).
[6] V. P. Kalosha and J. Herrmann, Phys. Rev. A **68**, 023812 (2003).
[7] S. A. Akhmanov, V. A. Vysloukh, and A. S. Chirkin, *Optics of Femtosecond Laser Pulses* (AIP, New York, 1992).
[8] G. P. Agrawal, *Nonlinear Fiber Optics* (Academic, San Diego, 1995).
[9] Yu. A. Shpolyanskiy, D. L. Belov, M. A. Bakhtin, and S. A. Kozlov, Appl. Phys. B: Lasers Opt. **77**, 349 (2003).
[10] V. G. Bespalov, S. A. Kozlov, and Yu. A. Shpolyanskiy, in *Proceedings of the International Conference LASERS 98* (STS Press, McLean, VA, 1999), pp. 1087–1092.
[11] A. Brodeur and S. L. Chin, J. Opt. Soc. Am. B **16**, 637 (1999).
[12] A. L. Gaeta, Phys. Rev. Lett. **84**, 3582 (2000).
[13] S. Tzortzakis, L. Sudrie, M. Franko, B. Prade, A. Mysyrowics, A. Couairon, and L. Berge, Phys. Rev. Lett. **87**, 213902 (2001).
[14] V. P. Kandidov, O. G. Kosareva, and A A Koltun, Quantum Electron. **33**, 69 (2001).
[15] A. N. Azarenkov, G. B. Altshuller, and S. A. Kozlov, *Huygens' Principle 1690–1990: Theory and Applications*, North-Holland (Studies in Mathematical Physics, Vol. 3 (North-Holland, Amsterdam, 1992), pp. 429–433.
[16] N. N. Rosanov, *Spatial Hysteresis and Optical Patterns* (Berlin, Springer, 2002), p. 308.
[17] A. N. Berkovskii, S. A. Kozlov, and Yu. A. Shpolyanskii, J. Opt. Technol. **69**, 163 (2002).
[18] S. A. Kozlov and P. A. Petroshenko, JETP Lett. **76**, 206 (2002).
[19] S. N. Vlasov and V. I. Talanov, *Self-Focusing of Waves* (Institute of Applied Physics of Russian Academy of Sciences, Nizhni Novgorod, 1997) (in Russuan).
[20] S. A. Izyurov and S. A. Kozlov, JETP Lett. **71**, 453 (2000).
[21] M. Born and E. Wolf, *Principles of Optics* (Pergamon Press, New York, 1968), p. 720.
[22] A. N. Azarenkov, G. B. Altshuler, N. R. Belashenkov, and S. A. Kozlov, Quantum Electron. **23**, 633 (1993).
[23] A. V. Husakou and J. Herrmann, Phys. Rev. Lett. **87**, 203901 (2001).
[24] J. N. Ames, S. Ghosh, R. S. Windeler, A. L. Gaeta, and S. T. Cundiff, Appl. Phys. B: Lasers Opt. **77**, 279 (2003).
[25] N. Blombergen, H. Lotem, and R. T. Lynch, Indian J. Pure Appl. Phys. **16**, 151 (1978).
[26] L. Sudrie, A. Couairon, M. Franco, B. Lamouroux, B. Prade, S. Tzortzakis, and A. Mysyrowich, Phys. Rev. Lett. **89**, 186601 (2002).
[27] M. B. Vinogradova, O. V. Rudenko, and A. P. Sukhorukov, *Wave Theory* (Science, Moscow, 1990), p. 432 (in Russian).
[28] E. M. Belenov and A. V. Nazarkin, JETP Lett. **53**, 188 (1991).
[29] S. A. Kozlov and S. V. Sazonov, JETP **84**, 221 (1997).
[30] S. A. Kozlov, Opt. Spectrosc. **84**, 887 (1998).
[31] A. O. Ukrainsky and S. A. Kozlov, J. Opt. B: Quantum Semiclassical Opt. **3**, 180 (2001).
[32] Th. Brabec and F. Krausz, Phys. Rev. Lett. **78**, 3282 (1997).
[33] J. K. Ranka and A. L. Gaeta, Opt. Lett. **23**, 534 (1998).
[34] A. A. Balakin and V. A. Mironov, JETP Lett. **75**, 617 (2002).
[35] A. T. Kaplan and P. L. Shkolnikov, Phys. Rev. Lett. **75**, 2316 (1995).